AD-A150 974   ELECTRON STIMULATED DESORPTION AND THE ROLE OF   1/1
               SECONDARY ELECTRONS(U) GEORGE WASHINGTON UNIV
               WASHINGTON D C DEPT OF CHEMISTRY F L HUTSON ET AL.
UNCLASSIFIED   NOV 84 TR-16 N00014-80-K-0852   F/G 7/4   NL

END
FILMED

DTIC
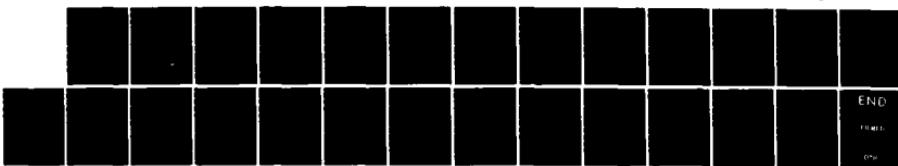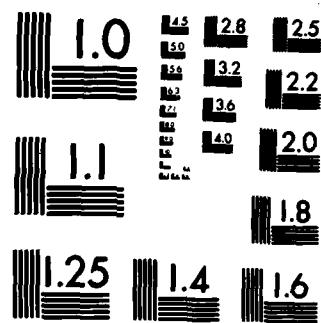
MICROCOPY RESOLUTION TEST CHART

NATIONAL BUREAU OF STANDARDS-1963-A

ELECTRON STIMULATED DESORPTION AND
THE ROLE OF SECONDARY ELECTRONS

By

F. L. Hutson, David E. Ramaker, V. M. Bermudez, and M. A. Hoffbauer

George Washington University
Department of Chemistry
Washington, D.C.   20052

November 1984

AD-A150 974

SELECT

MAR 6 1985

A

REPORT DOCUMENTATION PAGE		READ INSTRUCTIONS BEFORE COMPLETING FORM
1. REPORT NUMBER No. 16	2. GOVT ACCESSION NO.	3. RECIPIENT'S CATALOG NUMBER
4. TITLE (and Subtitle) ELECTRON STIMULATED DESORPTION AND THE ROLE OF BACKSCATTERED ELECTRONS		5. TYPE OF REPORT & PERIOD COVERED Technical Report
		6. PERFORMING ORG. REPORT NUMBER
7. AUTHOR(s) F. L. Hutson, D. E. Ramaker, V. M. Bermudez and M. A. Hoffbauer		8. CONTRACT OR GRANT NUMBER(s) N00014-80-K-0852
9. PERFORMING ORGANIZATION NAME AND ADDRESS Chemistry Department George Washington University Washington, D.C. 20052		10. PROGRAM ELEMENT, PROJECT, TASK AREA & WORK UNIT NUMBERS Prog. Elem. No. 61153N Task Area No. PP 013-08-01 Work Unit # NR 056-681
11. CONTROLLING OFFICE NAME AND ADDRESS Office of Naval Research, Dept. of Navy 800 N. Quincy Street Washington, D.C. 22217		12. REPORT DATE Nov. 1984
		13. NUMBER OF PAGES 18
14. MONITORING AGENCY NAME & ADDRESS(If different from Controlling Office)		15. SECURITY CLASS. (of this report) Unclassified
		15a. DECLASSIFICATION/DOWNGRADING SCHEDULE

16. DISTRIBUTION STATEMENT (of this Report)

This document has been approved for public release and sale; its distribution is unlimited.

17. DISTRIBUTION STATEMENT (of the abstract entered in Block 30, if different from Report)

19. KEY WORDS (Continue on reverse side if necessary and identify by block number)

Electron Stimulated desorption, secondary electrons, electron loss spectroscopy.

20. ABSTRACT (Continue on reverse side if necessary and identify by block number)

Electron stimulated desorption (ESD) yields of ions and neutrals from surfaces are expected to contain large contributions due to backscattered electrons from the bulk. A procedure for deconvoluting these effects from experimental yield data has been developed which included contributions from both true secondaries and backscattered primaries. The procedure allows for changes in the backscattered yield with primary energy which is particularly necessary at low primary energies (10-40 eV) where most ESD thresholds occur. This method is applied to recently published excited OH neutral (OH*) yields from TiO₂. Although this

deconvolution procedure reveals significant contributions from backscattered electrons, more importantly it also indicates that a significant yield arises from a direct non-resonant excitation mechanism and not from secondary electrons. The resonant portion of the OH^+ yield curve from TiO_2 is found to be similar to published O^- ESD data from O/W and O/Mo.

Accession For

NTIS	GRA&I	☑
DTIC	TAB	
Unannounced		
Justification		

| Distribution/ |
| Availability Codes |
	Avail and/or
Dist	Special
A-1	
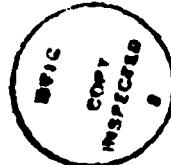
DTIC COPY INSPECTED

1. INTRODUCTION

Recent reports on the extent of secondary electron contributions in electron/photon stimulated desorption (ESD/PSD) appear to be contradictory. Jaeger et al. (1) suggested that secondary electrons provided the dominant contribution to the H^+ yield from NH_3/Ni and called the process x-ray induced ESD (XESD). Others have concluded that the XESD process is the dominant mechanism in the PSD of N^+ and O^+ ions from mixed condensed gases such as N_2-O_2 (2) and in the PSD of H^+ ions from H_2/YbO_x-Sm (3). On the other hand, large differences were found between the secondary electron yield and the PSD O^+ yield from O/Cr providing strong evidence for the domination of a direct photon excitation mechanism (4). A similar conclusion was reached for the PSD of H^+ ions from OH/Ti, Cr, and Cu (5). Finally, a comparison of the ESD O^+ yield from NO/Pt (110), originating from molecularly adsorbed NO, revealed that the O^+ yield begins only at the O K level and indicates that only a direct core level process is active (6).

One can make attempts to explain some of these apparently conflicting reports. The evidence cited above claiming a dominant XESD role could possibly be explained by other mechanisms (e.g., resonant hole delocalization (6) in N_2/O_2). The apparent absence of the XESD mechanism in other systems might be explained by the low core levels studied in some of these systems. For example, the Ti, Cr, and Cu 3p core levels studied above have binding energies of only 30 to 80 eV compared to the deeper N and O K levels around 400-550 eV. Regardless of the explanation, the actual magnitude of the secondary electron contribution in the ESD/PSD process is clearly not known.

Qualitative estimates of the secondary electron contributions to the desorption yield can be made. If a valence excitation mechanism provides a large desorption cross section, one expects to see secondary electrons play a signifi-

ELECTRON STIMULATED DESORPTION AND THE ROLE OF BACKSCATTERED ELECTRONS

F.L. Hutson[*]
Department of Chemistry
George Washington University
Washington, DC 20052

and

D.E. Ramaker, V.M. Bermudez and M.A. Hoffbauer[+]
Naval Research Laboratory
Washington, DC 20375

Electron stimulated desorption (ESD) yields of ions and neutrals from surfaces are expected to contain large contributions due to backscattered electrons from the bulk. A procedure for deconvoluting these effects from experimental yield data has been developed which includes contributions from both true secondaries and backscattered primaries. The procedure allows for changes in the backscattered yield with primary energy which is particularly necessary at low primary energies (10-40 eV) where most ESD thresholds occur. This method is applied to recently published excited OH neutral (OH^*) yield from TiO_2. Although this deconvolution procedure reveals significant contributions from backscattered electrons, more importantly it also indicates that a significant yield arises from a direct non resonant excitation mechanism and not from secondary electrons. The resonant portion of the OH^* yield curve from TiO_2 is found to be similar to published O^-, ESD data from O/W and O/Mo. Originator Supplied Keywords include:

(Several/PLUS 19)

cant role at deeper core level energies. One also expects that systems with very low desorption thresholds should exhibit large secondary desorption yields due to the large number of secondary electrons at very low energy. Thus neutral or negative ion desorption yields, which reveal lower desorption thresholds than positive ions, should exhibit even larger secondary electron effects.

In this work we examine the secondary electron contributions to the excited OH neutral (OH*) yield from TiO_2 as recently reported by Bermudez and Hoffbauer (7). This ESD desorption yield has a sharp threshold at 11 eV relative to the Fermi level. We report the first attempt at quantitatively determining the secondary electron contribution by deconvoluting the backscattered electron spectrum from the measured ESD OH* yield. The deconvoluted spectrum allows for semi-quantitative interpretation of the ESD spectrum and thus provides for a determination of the various mechanisms involved in the excited neutral desorption process. A detailed interpretation of the ESD OH* yield from TiO_2 is reported elsewhere (8). In Sec. 2 we describe the details of our procedure for obtaining a backscattered spectrum as a function of primary energy. Results and a discussion are presented in Sec. 3.

2. THE BACKSCATTERED SPECTRUM

The procedure for substraction or deconvolution of electron energy loss effects from an Auger or photoelectron lineshape is well known (9). The expression,

$$N(E) = \int L(E_p,\epsilon)N_t(\epsilon)d\epsilon, \qquad (1)$$

mathematically describes this relationship between $N(E)$, the experimentally measured spectrum, and $N_t(E)$, the "true" or undistorted spectrum. The "response" function, $L(E_p,\epsilon)$, is usually obtained from the backscattered or loss spectrum

where the primary energy E_p is chosen to be near the principal peak of the spectrum $N(E)$. The deconvolution in Auger spectroscopy has normally been accomplished using the van Cittert iteration procedure, although Fourier analysis techniques have also been used (9).

The loss spectrum, $L(E_p,\epsilon)$, can be characterized as having true secondary, $SEC(E_p,\epsilon)$, redistributed primary, $RP(E_p,\epsilon)$, and elastically scattered, $ES(E_p)$, contributions,

$$L(E_p,\epsilon) = A(E_p)SEC(E_p,\epsilon) + B(E_p)RP(E_p,\epsilon) + ES(E_p) \qquad (2)$$

Expressions for SEC and RP have been derived previously from theoretical analysis of the secondary cascade process and the Bethe expression for electron scattering (9),

$$SEC(E_p,\epsilon) = \epsilon/[(\epsilon+E_o)(\epsilon+\phi)^m] \qquad (3)$$

$$RP(E_p,\epsilon) = \ell n[(E_p-\epsilon)/E_b]/[(E_p-\epsilon)/E_b]^n \qquad (4)$$

The expression for SEC is essentially the Sickafus (10) expression $(\epsilon + \phi)^{-m}$ multiplied by an escape factor $(\epsilon/(\epsilon + E_o))$, where ϕ and E_o are the work function and the escape probability parameters respectively. Here E_o was chosen (9) to be 0.5. In RP, E_p and E_b are the primary electron beam energy and the effective binding energy of the valence band. The expressions for SEC and RP of course do not reproduce any structure arising from Auger and characteristic energy losses; thus, they approximate only the overall envelope of $L(E_p,\epsilon)$. ES is generally Gaussian in shape, the width determined by the resolution of the electron analyzer. $A(E_p)$ and $B(E_p)$ are coefficients which depend on primary energy and relate the size of the secondary and redistributed primary contributions relative to the elastically scattered peak.

With the differences noted below, Eq. (1) also describes the relationship between the measured and "true" ESD yield. However, two factors make the ESD situation significantly more difficult than in the Auger case. First, the Auger

3

electron energies are usually well above 50 eV, in which case, one can ignore SEC as well as the variation in $B(E_p)$ so that $L(E_p,\varepsilon)$ can be approximated as $B[RP(E_p-\varepsilon)]$. Second, $N_t(E)$ should theoretically go to zero well below the main Auger features, so B is usually determined consistent with this criterion (9). The ESD OH[*] yield has a threshold at 11 eV and its behavior at higher energies, in the absence of contributions from secondaries, is not generally known. Thus, knowledge of $SEC(E_p,\varepsilon)$, $A(E_p)$ and $B(E_p)$ is required.

The proper choice of A and B is complicated by the nature of the ESD process itself. Desorption may arise from both the incoming electrons, having total current I_p, as well as from the outgoing electrons as they travel through the outer surface layer, where all desorption is assumed to originate. This is in contrast to the Auger lineshape where the entire signal results from escaping electrons. Thus the appropriate choice for A and B cannot be determined directly from the experimentally measured backscattered spectrum, but rather must be related to the total yield,

$$\delta(E_p) = \int_0^{E_p} [L(E_p,\varepsilon)/I_p(E_p)]d\varepsilon, \qquad (5)$$

and the ratio of total secondaries to redistributed primaries,

$$R(E_p) = A(E_p)\int_0^{E_p} SEC(E_p,\varepsilon)d\varepsilon / [B(E_p)\int_0^{E_p} RP(E_p,\varepsilon)d\varepsilon]. \qquad (6)$$

Knowledge of R and δ allows A and B to be calculated.

The measurement of δ is usually accomplished by collecting all of the backscattered electrons over all angles and energies (11). As an alternate procedure (12), adequate at higher energies (e.g., $E_p = 50$ to 100 eV), one can measure the current through an electrometer to ground when the sample is biased to a relatively large positive voltage, V_o (e.g., $V_o = +300$ V_{DC}) and when the sample is biased slightly negative (e.g., $V_1 = -6$ V_{DC}). δ can then be calculated from the expression,

4

$$\delta = (I(V_0) - I(V_1))/I(V_0), \tag{7}$$

which assumes that $I(V_0)$ equals I_p and $I(V_0) - I(V_1)$ equals the total backscattered spectrum. Eq. (7) thus assumes that the backscattered electron yield above the energy eV_0 is negligible (i.e., that the secondary electron contribution is much larger than the redistributed primary and elastically scattered contribution, which of course is valid only at higher energies).

Our need for R as well as δ suggested a third procedure for measuring δ. We recorded the backscattered spectrum from OH/TiO_2 (prepared exactly as in the ESD experiments (7)) at 15 values of Ep (50 to 200 eV at 10 eV intervals) using a single-pass cylindrical mirror analyzer (CMA) equipped with a "Spiraltron" electron multiplier (Bendix 4219). Spectra were recorded in both the $d[EN(E)]/dE$ mode, using lock-in detection with I_p ~0.3-1.22 µA, and the $EN(E)$ mode using pulse-counting with I_p ~1-8 nA. A correction for the dependence of the detector gain on energy was applied to the data using the results of Arnoldy et al. (13) assuming electron impact on the front-end cone of the multiplier. Integration of the spectrum allows δ to be calculated from Eq. (5). I_p was determined as above (i.e., $I_p = I(V_0)$) and δ was normalized so that the maximum value (δ_{max}), which occurred at ~200 eV, was equal to that measured directly as in Eq. (7), δ_{max} ~1.2. The normalization is required since, of course, the CMA collects only a fraction of the total scattered electrons (i.e., only those entering the narrow acceptance angle of the CMA). This procedure is valid provided the backscattered spectrum is reasonably isotropic. One advantage of this procedure is that it eliminates the problem at low energies inherent in Eq. (7), where $I(V_0)$ and $I(V_1)$ are both small.

It is considerably more difficult to determine R, and to our knowledge no reports of R appear in the literature. We separated the SEC and RP contributions by fitting the expressions in Eqs. (3) and (4) to the total loss spectrum measured

at 180 eV. Differences between the fit and the experimental spectrum were then added to one or the other contributions (e.g., Auger structure around 20 eV was added to the SEC contribution and the characteristic loss structure around ΔE -30 eV as added to RP). The resultant contributions are shown in Fig. (1). The separation into SEC and RP at lower energies was accomplished by fitting the separated contributions at 180 eV to the measured spectrum as suggested by Eq. (2). The RP contribution was moved along the energy scale in each case since it depends on $E_p - \epsilon$; the SEC contribution was not moved in energy. Fig. (1) illustrates at 80 and 140 eV the remarkably good fits which were achieved throughout the energy range 50-170 eV.

Data below 50 eV could not be obtained for either δ or R because of focussing problems and a decreasing gun current. In order to assist us in an extrapolation down to 11 eV, we made use of some backscattered spectra below 50 eV found for MgO (14). In fact, to the best of our knowledge these are the only yield and loss spectral data below 50 eV available for any material. The MgO data below 30 eV were taken with a LEED system; thus, all backscattered electrons were collected for the determination of δ (15). Fig. (2) shows the yield curve obtained below 30 eV from an epitaxial MgO layer on Mo. These data are compared with δ obtained from Eq. (7) above 50 eV from a similar MgO/Mo sample, and with $\delta*4.5$ obtained by integra-tion of $L(E_p, \epsilon)$ from OH/TiO$_2$ as described above. The factor of 4.5 simply accounts for the higher yield of MgO, but the variation with energy is surprisingly similar. A comparison is shown of the experimental curves with a "universal" curve fit

$$\delta = e^2 \delta_{max}(E_p/E_{max}) \exp[-2(E_p/E_{max})^{1/2}] \tag{8}$$

proposed by Sternglass (11,16) to represent the yield function with E_p. Clearly Eq. (8) overestimates δ below E_{max}. The structure in δ below 30 eV apparently arises from diffraction (15).

6

Results for δ and R are shown in Fig. (3). Those above 50 eV are obtained
from OH/TiO$_2$; those below 50 eV are extrapolated using the behavior of the MgO/Mo
data as a guide. The backscattered data from MgO/Mo shows that R gets very large
as E_p approaches zero. This may simply be due to our choice of division into SEC
and RP, which becomes rather arbitrary at very low energies. Some structure may
be indicated in R around 100 eV, but we have drawn the best smooth curve through
the points. Any structure would not be critical in the deconvolution process, and
the smooth curve allows us to extrapolate to lower energy consistent with the
MgO/Mo data. These R and δ curves were utilized along with Eqs. (1) and (2) to
deconvolute the ESD OH* yield data from OH/TiO$_2$. Since the resolution of the ESD
spectra is limited only by the thermal energy spread of the electron gun ($\sim$0.5
eV), the experimental ES was replaced by a gaussian of 0.5 eV width but with the
same area.

3. RESULTS AND DISCUSSION

Deconvolution of the measured ESD OH* yield, as shown in Fig. (4), indicates
that the yield intensity above 50 eV is not due entirely to backscattered
electrons. This indicates that a direct nonresonant excitation is partly
responsible for the intensity above 50 eV. A detailed comparison, reported
elsewhere (8), of the OH$^+$ and H$^+$ yields (17) reveals that the OH$^+$ yield reflects
primarily the nonresonant cross section. Fig. (4) indicates that the OH* yield
results from both resonant and nonresonant excitations.

Secondary electrons may of course produce desorption via both the resonant
and nonresonant mechanisms. However, the resonant portion has a finite width with
some structure; thus, the secondary electron contributions may more visibly
distort the resonant portion than the nonresonant portion. The latter is
relatively smooth and extends indefinitely to higher energy. Thus we substracted
the experimental OH$^+$ yield shown in Fig. (5) (it reflects the nonresonant portion

with its secondary electron contributions) from the OH* yield, leaving the resonant portion with its secondary electron contribution (the latter is also shown in Fig. (5)). In this subtraction procedure, the relative OH* and OH$^+$ intensities are fixed so that the deconvoluted resonant portion goes to zero at higher energies as one would expect for a resonant excitation.

Comparison of the resonant OH* yield with the total O$^-$ yield from O/Mo and O/W (18) reveals some similarity in the spectra. This suggests that the O$^-$ desorption yield results predominantly from resonant excitations and that the resonant excitations are similar for O/Mo or W and for OH/TiO$_2$.

Specific electron assignments to the various peaks have been suggested and reported elsewhere (8). Briefly, the three features around 17, 25 and 35 eV in the OH* yield are believed to result from totally resonant electron attachment, i.e., $3a_1^{-1}3d^{*2}$, $3a_1^{-1}3d^*v^*$ and $3a_1^{-1}v^{*2}$ excitations, where $3d^*$ and v^* are antibonding orbitals or resonances in the conduction band and $3a_1$ is a σ bonding OH orbital (19). The corresponding features in the O$^-$ yields arise from similar excitations out of the O 2p orbitals. The intensity around 50 eV is believed to arise from a resonant electron attachment $3p^{-1}v^*4a_1$ followed by an Auger decay to the $v^{-2}v^*4a_1$ configuration, which initiates the desorption. The 3p core levels of Ti, Mo, and W all fall around 35 eV (20,21). The direct nonresonant OH* yield apparently arises from a nonresonant $3p^{-1}$ core excitation or ionization plus shakeup. A 2 hole-1 electron final state in either case can initiate the OH* desorption.

In conclusion, this work has shown a significant secondary electron contribution to the ESD OH* yield. More importantly, the results indicate that the yield above 50 eV is not due entirely to secondary electrons. Rather a significant yield also arises from a direct nonresonant excitation in apparent contrast to the O$^-$ yield from O/Mo and W. Deconvolution of the resonant portion enables semi-quantitative interpretation of the spectrum (8).

8

9

References

1. R. Jaeger and J. Stöhr and T. Kendelewicz, Phys. Rev. B28, 1145 (1983).

2. C.C. Parks, R.A. Rosenberg, P.J. Love, P.R. LaRoe and V. Rehn, Phys. Rev. B31, xxx (1985) to be published.

3. J. Schmidt-May, C. Kunz and F. Senf in "Desorption Induced by Electronic Transitions (DIET II)", edited by W. Brenig and D. Menzel, (Springer, Heidelberg, 1985) to be published.

4. E. Bertel, R. Stockbauer, R.L. Kurtz, D.E. Ramaker and T.E. Madey, submitted to Phys. Rev. B.

5. D.E. Ramaker, E. Bertel, R.L. Kurtz, R. Stockbauer and T.E. Madey, submitted to Phys. Rev. B.

6. U. Schwalke, H. Niehus and G. Comsa, Surf. Sci. 137, 23 (1984).

7. V.M. Bermudez and M.A. Hoffbauer, Phys. Rev. B30, 1125 (1984).

8. D.E. Ramaker in "Desorption Induced by Electronic Transitions (DIET II)", edited by W. Brenig and D. Menzel (Springer, Heidelberg, 1985) to be published.

9. D.E. Ramaker, J.S. Murday and N.H. Turner, J. Electron Spect. Related Phen. 17, 45 (1979).

10. E.N. Sickafus, Rev. Sci. Instrum. 42, 933 (1971); Phys. Rev. B16, 1436 (1977).

11. O. Hachenberg an W. Brauer, "Adv. Electronics and Electron Physics" 11, edited by L. Marton and C. Marton (Academic, NY, 1959), p. 413.

12. J.W. Gibson and R.E. Thomas, Applic. Surf. Sci. 14, 56 (1982).

13. R.L. Arnoldy, P.O. Isaacson, D.F. Gats and L.W. Choy, Rev. Sci. Instrum. 44, 172 (1973).

14. R.E. Thomas, private communication.

15. R.E. Thomas, J.W. Gibson and G.A. Haas, Applic. Surf. Sci. 5, 398 (1980).

16. E.J. Sternglass, Westinghouse Research Lab. Sci. Paper No. 1772 (1954).

17. M.L. Knotek, Surf. Sci. 101, 334 (1980).

18. Z.X. Liu and D. Lichtman, Surf. Sci. 114, 287 (1982).

19. T. Kawai, M. Tsukada, H. Adachi, C. Satoko and T. Sakata, Surf. Sci. 81, L640 (1979).

20. T.E. Madey, R. Stockbauer, J.F. Van der Veen and D.E. Eastman, Phys. Rev. Lett. 45, 187 (1980).

21. R. Jaeger, J. Stöhr, J. Feldhaus, S. Brennan and D. Menzel, Phys. Rev. B23, 2102 (1981)

Figure Captions

1. Comparison of the measured backscattered spectrum for OH/TiO$_2$ at primary energy E_p = 140 eV (top) and 80 eV (bottom) to the best fit of Eq. (2). In Eq. (2), SEC(ϵ) and RP(E_p,ϵ) were obtained from the E_p = 180 eV backscattered spectrum where the separation into SEC and RP is described in the text.

2. Top: The measured total electron yield from a 35 Å epitaxial MgO film on Mo as reported in refs. 12 and 15. The δ below 30 eV was obtained by collecting the total backscattered current; that above 30 eV was measured utilizing Eq. (7). Also shown is δ≈4.5 obtained in this work for OH/TiO$_2$ by integrating L(E_p,ϵ) and normalizing as described in the text. The dashed line is a fit of Eq. (8) to the total MgO/Mo yield.

   Bottom: Comparison of the "universal curve" with experiment over a broad energy range.

3. Plot of R and δ as defined in Eqs. (5) and (6) respectively and determined as described in the text.

4. Comparison of the measured ESD OH* yield for OH/TiO$_2$ with the deconvoluted OH* yield.

5. Top: Comparison of the ESD OH* yield for OH/TiO$_2$ (ref. 7)) with the OH$^+$ yield (ref. 16)). The resonant OH* yield, as obtained by subtraction of the above two curves, and the deconsoluted resonant OH* are also shown.

   Bottom: The ESD O$^-$ yield from O/W and O/Mo as reported by Liu and Lichtman (ref. 18) is compared with the resonant OH* yield from Fig. 4.

Fig. 1

TOTAL e⁻ YIELD

Theory, Eq. (8)

MgO/Mo

MgO/Mo

OH/TiO$_2$

YIELD

0   25   50   75   100   125

Theory, Eq. (8)

Exp., MgO/Mo

YIELD

0   250   500   750   1000   1250   1500

ELECTRON ENERGY (EV)

Fig.

ESD, OH/TiO$_2$

Total

Deconvoluted

ELECTRON ENERGY (EV)

YIELD

ESD, OH/TiO$_2$

Total OH*

OH$^+$

Res. OH*

Decon. Res. OH*

YIELD

O$^-$ – O/W

O$^-$ – O/Mo

OH* – OH/TiO$_2$

YIELD

ELECTRON ENERGY (EV)

Fi<
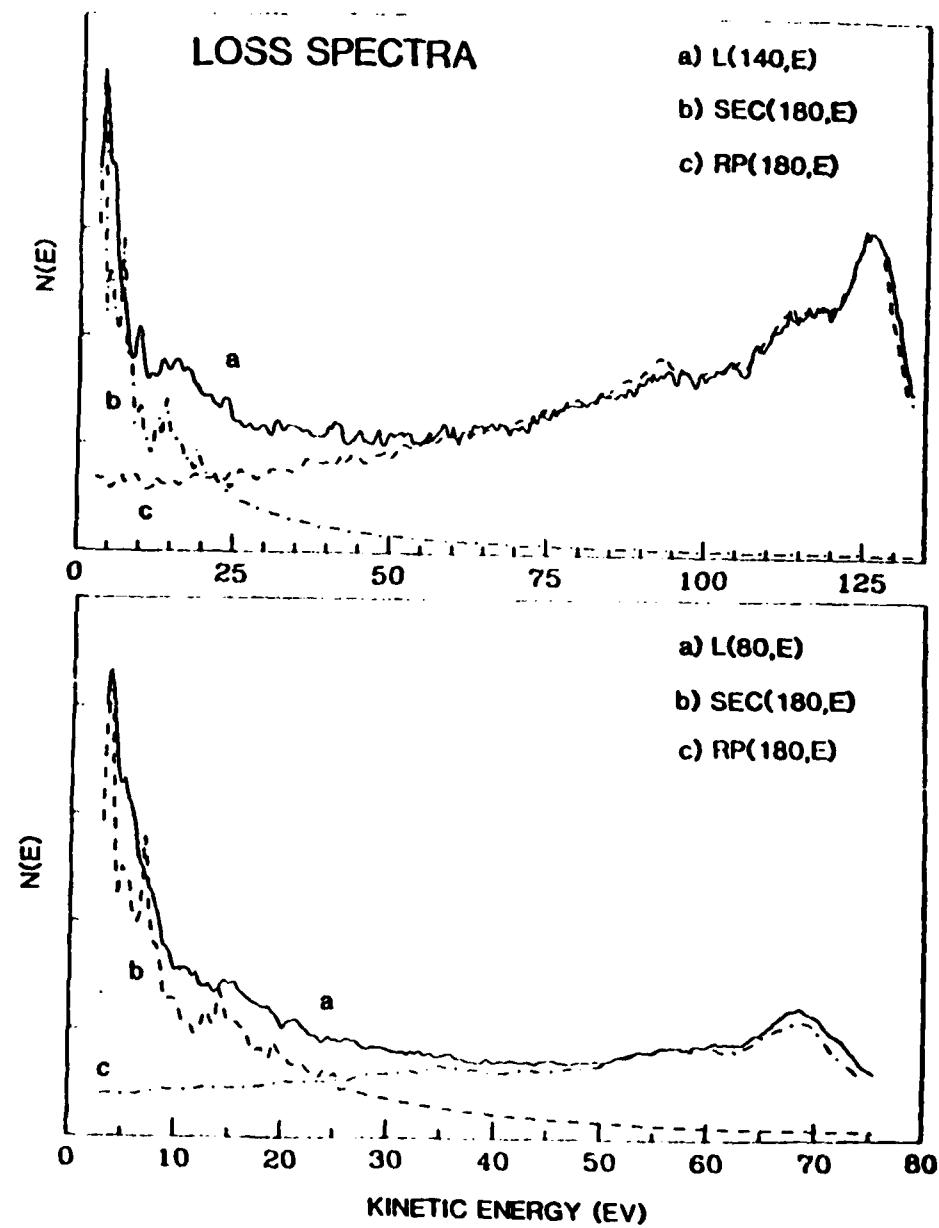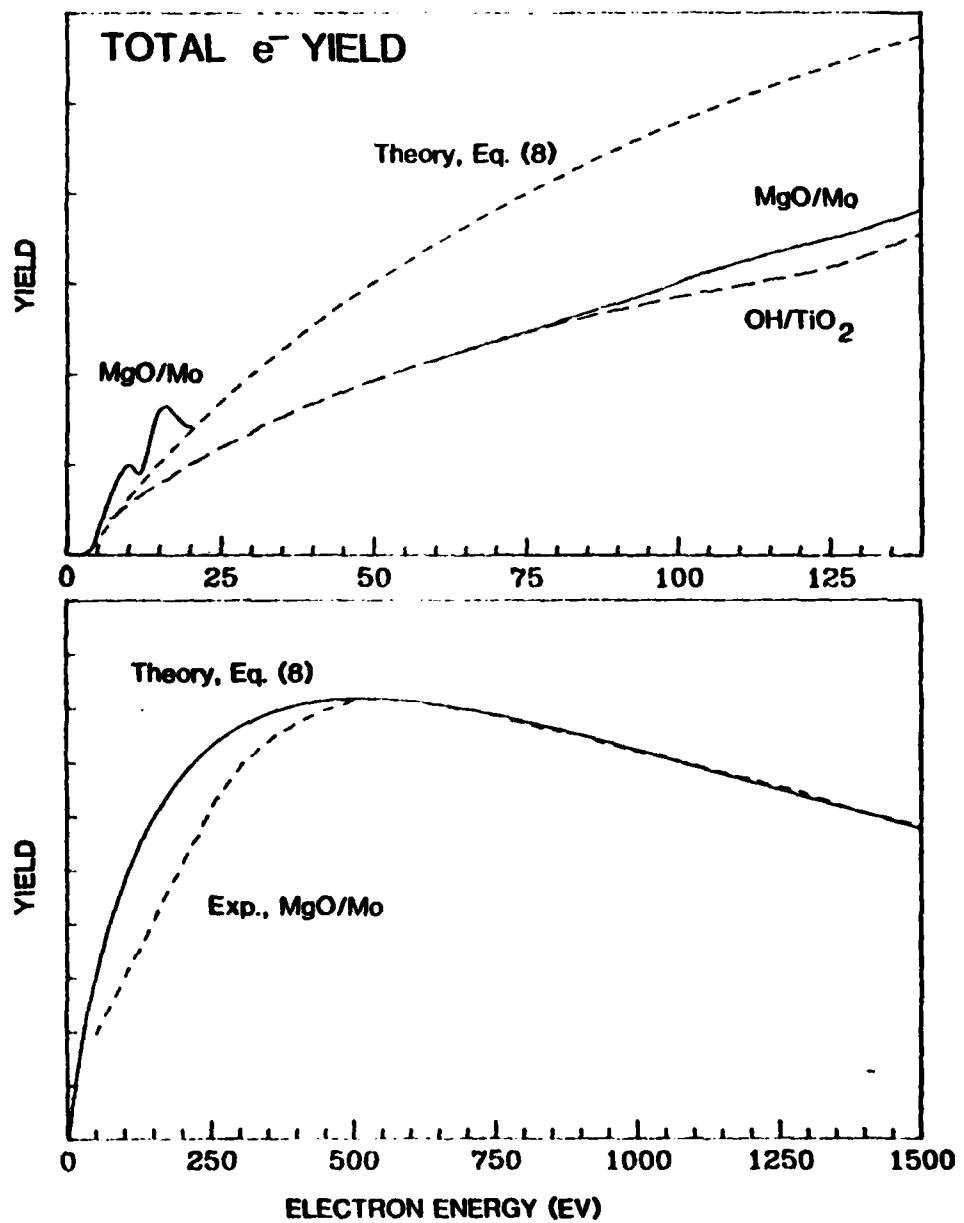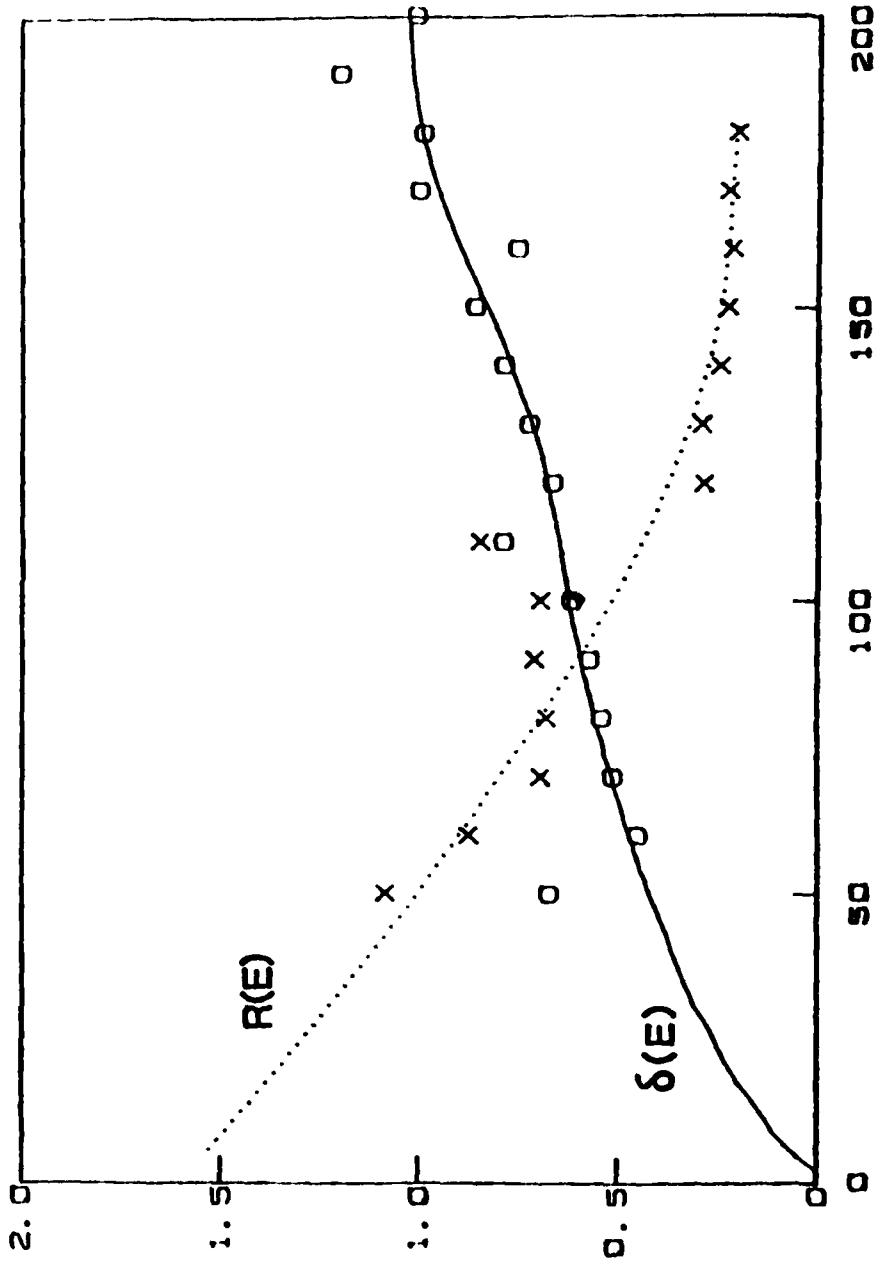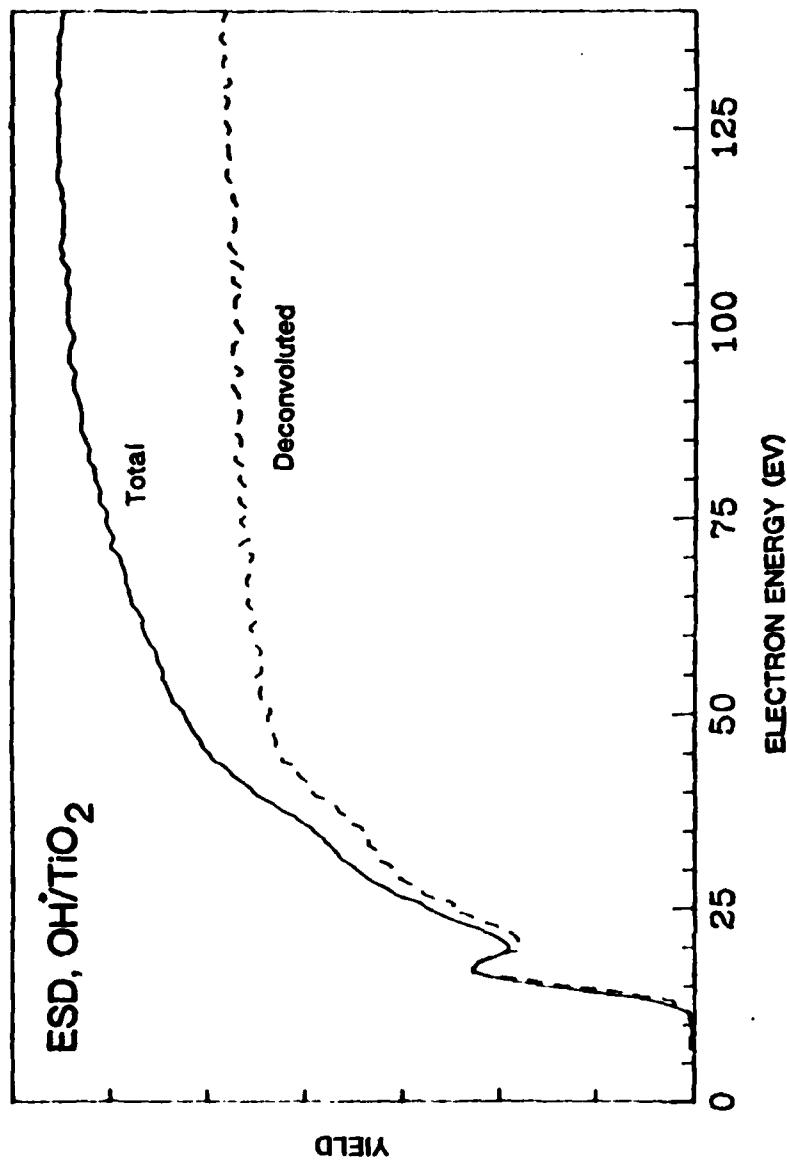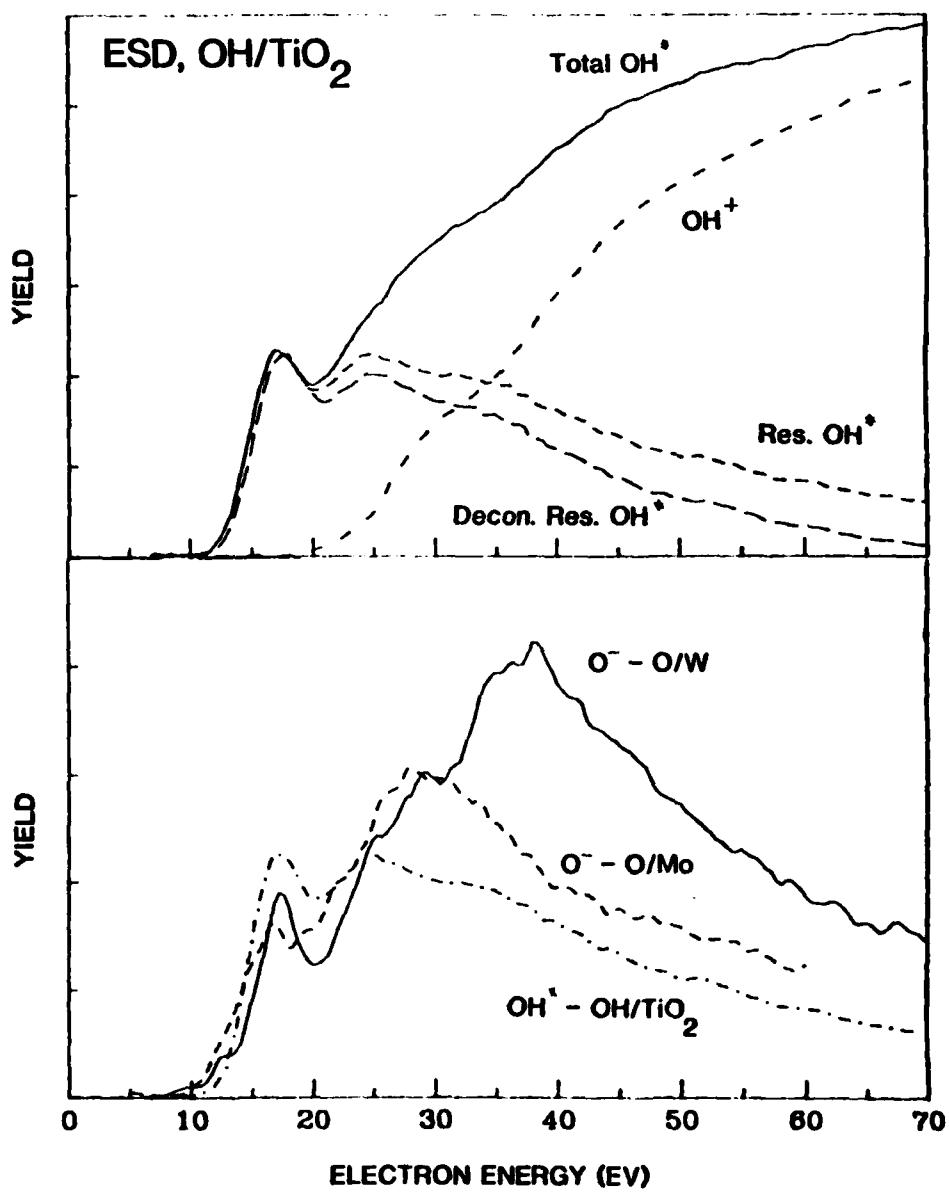
DL/413/83/01
GEN/413-2

TECHNICAL REPORT DISTRIBUTION LIST, GEN

	No. Copies		No. Copies
Office of Naval Research Attn: Code 413 800 N. Quincy Street Arlington, Virginia 22217	2	Dr. David Young Code 334 NORDA NSTL, Mississippi 39529	1
Dr. Bernard Douda Naval Weapons Support Center Code 5042 Crane, Indiana 47522	1	Naval Weapons Center Attn: Dr. A. B. Amster Chemistry Division China Lake, California 93555	1
Commander, Naval Air Systems Command Attn: Code 310C (H. Rosenwasser) Washington, D.C. 20360	1	Scientific Advisor Commandant of the Marine Corps Code RD-1 Washington, D.C. 20380	1
Naval Civil Engineering Laboratory Attn: Dr. R. W. Drisko Port Hueneme, California 93401	1	U.S. Army Research Office Attn: CRD-AA-IP P.O. Box 12211 Research Triangle Park, NC 27709	1
Defense Technical Information Center Building 5, Cameron Station Alexandria, Virginia 22314	12	Mr. John Boyle Materials Branch Naval Ship Engineering Center Philadelphia, Pennsylvania 19112	1
DTNSRDC Attn: Dr. G. Bosmajian Applied Chemistry Division Annapolis, Maryland 21401	1	Naval Ocean Systems Center Attn: Dr. S. Yamamoto Marine Sciences Division San Diego, California 91232	1
Dr. William Tolles Superintendent Chemistry Division, Code 6100 Naval Research Laboratory Washington, D.C. 20375	1		

ABSTRACTS DISTRIBUTION LIST, 056/625/629

Dr. F. Carter
Code 6132
Naval Research Laboratory
Washington, D.C. 20375

Dr. Richard Colton
Code 6112
Naval Research Laboratory
Washington, D.C. 20375

Dr. Dan Pierce
National Bureau of Standards
Optical Physics Division
Washington, D.C. 20234

Dr. R. Stanley Williams
Department of Chemistry
University of California
Los Angeles, California 90024

Dr. R. P. Messmer
Materials Characterization Lab.
General Electric Company
Schenectady, New York 22217

Dr. Robert Gomer
Department of Chemistry
James Franck Institute
5640 Ellis Avenue
Chicago, Illinois 60637

Dr. Ronald Lee
R301
Naval Surface Weapons Center
White Oak
Silver Spring, Maryland 20910

Dr. Paul Schoen
Code 5570
Naval Research Laboratory
Washington, D.C. 20375

Dr. John T. Yates
Department of Chemistry
University of Pittsburgh
Pittsburgh, Pennsylvania 15260

Dr. Richard Greene
Code 5230
Naval Research Laboratory
Washington, D.C. 20375

Dr. L. Kesmodel
Department of Physics
Indiana University
Bloomington, Indiana 47403

Dr. K. C. Janda
California Institute of Technology
Division of Chemistry and Chemical
  Engineering
Pasadena, California 91125

Dr. E. A. Irene
Department of Chemistry
University of North Carolina
Chapel Hill, Northc Carolina 27514

Dr. Adam Heller
Bell Laboratories
Murray Hill, New Jersey 07974

Dr. Martin Fleischmann
Department of Chemistry
Southampton University
Southampton S09 5NH
Hampshire, England

Dr. John W. Wilkins
Cornell University
Laboratory of Atomic and
  Solid State Physics
Ithaca, New York 14853

Dr. Richard Smardzewski
Code 6130
Naval Research Laboratory
Washington, D.C. 20375

Dr. H. Tachikawa
Chemistry Department
Jackson State University
Jackson, Mississippi 39217

DL/413/83/01
056/413-2

ABSTRACTS DISTRIBUTION LIST, 056/625/629

Dr. R. G. Wallis
Department of Physics
University of California
Irvine, California 92664

Dr. R. W. Plummer
Department of Physics
University of Pennsylvania
Philadelphia, Pennsylvania 19104

Dr. D. Ramaker
Chemistry Department
George Washington University
Washington, D.C. 20052

Dr. E. Yeager
Department of Chemistry
Case Western Reserve University
Cleveland, Ohio 41106

Dr. J. C. Hemminger
Chemistry Department
University of California
Irvine, California 92717

Dr. N. Winograd
Department of Chemistry
Pennsylvania State University
University Park, Pennsylvania 16802

Dr. T. F. George
Chemistry Department
University of Rochester
Rochester, New York 14627

Dr. G. D. Stein
Mechanical Engineering Department
Northwestern University
Evanston, Illinois 60201

Dr. G. Rubloff
IBM
Thomas J. Watson Research Center
P.O. Box 218
Yorktown Heights, New York 10598

Dr. A. Steckl
Department of Electrical and
  Systems Engineering
Rensselaer Polytechnic Institute
Troy, NewYork 12181

Dr. Horia Metiu
Chemistry Department
University of California
Santa Barbara, California 93106

Dr. G. H. Morrison
Department of Chemistry
Cornell University
Ithaca, New York 14853

Captain Lee Myers
AFOSR/NC
Bollig AFB
Washington, D.C. 20332

Dr. P. Hansma
Physics Department
University of California
Santa Barbara, California 93106

Dr. J. T. Keiser
Department of Chemistry
University of Richmond
Richmond, Virginia 23173

Dr. J. Baldeschwieler
California Institute of Technology
Division of Chemistry
Pasadena, California 91125

Dr. Roald Hoffmann
Department of Chemistry
Cornell University
Ithaca, New York 14853

Dr. W. Goddard
California Institute of Technology
Division of Chemistry
Pasadena, California 91125

Dr. J. E. Jensen
Hughes Research Laboratory
3011 Malibu Canyon Road
Malibu, California 90265

Dr. W. Knauer
Hughes Research Laboratory
3011 Malibu Canyon Road
Malibu, California 90265

Dr. J. H. Weaver
Department of Chemical Engineering
  and Materials Science
University

Dr. C. B. Harris
Department of Chemistry
University of California

ABSTRACTS DISTRIBUTION LIST, 056/625/629

Dr. F. Carter
Code 6132
Naval Research Laboratory
Washington, D.C. 20375

Dr. Richard Colton
Code 6112
Naval Research Laboratory
Washington, D.C. 20375

Dr. Dan Pierce
National Bureau of Standards
Optical Physics Division
Washington, D.C. 20234

Dr. R. Stanley Williams
Department of Chemistry
University of California
Los Angeles, California 90024

Dr. R. P. Messmer
Materials Characterization Lab.
General Electric Company
Schenectady, New York 22217

Dr. Robert Gomer
Department of Chemistry
James Franck Institute
5640 Ellis Avenue
Chicago, Illinois 60637

Dr. Ronald Lee
R301
Naval Surface Weapons Center
White Oak
Silver Spring, Maryland 20910

Dr. Paul Schoen
Code 5570
Naval Research Laboratory
Washington, D.C. 20375

Dr. John T. Yates
Department of Chemistry
University of Pittsburgh
Pittsburgh, Pennsylvania 15260

Dr. Richard Greene
Code 5230
Naval Research Laboratory
Washington, D.C. 20375

Dr. L. Kesmodel
Department of Physics
Indiana University
Bloomington, Indiana 47403

Dr. K. C. Janda
California Institute of Technology
Division of Chemistry and Chemical
  Engineering
Pasadena, California 91125

Dr. E. A. Irene
Department of Chemistry
University of North Carolina
Chapel Hill, Northc Carolina 27514

Dr. Adam Heller
Bell Laboratories
Murray Hill, New Jersey 07974

Dr. Martin Fleischmann
Department of Chemistry
Southampton University
Southampton S09 5NH
Hampshire, England

Dr. John W. Wilkins
Cornell University
Laboratory of Atomic and
  Solid State Physics
Ithaca, New York 14853

Dr. Richard Smardzewski
Code 6130
Naval Research Laboratory
Washington, D.C. 20375

Dr. H. Tachikawa
Chemistry Department
Jackson State University
Jackson, Mississippi 39217

END

FILMED

4-85

DTIC